Journal of Power Sources 189 (2009) 702–705

Contents lists available at ScienceDirect

Journal of Power Sources

journal homepage: www.elsevier.com/locate/jpowsour

Short communication

Intermittent X-ray diffraction study of kinetics of delithiation in nano-scale $LiFePO_4$

Jacob L. Jones, Jui-Ting Hung, Ying S. Meng*

Materials Science and Engineering, University of Florida, Gainesville, FL 32611-6400, United States

ARTICLE INFO

Article history:
Received 29 July 2008
Received in revised form 20 August 2008
Accepted 21 August 2008
Available online 28 August 2008

Keywords:
Lithium battery
LiFePO4
Kinetics
X-ray diffraction
Chemical delithiation

ABSTRACT

Using intermittent X-ray diffraction, an understanding of the time dependence of phase evolution in the electrode materials during lithium extraction can be determined. Phase evolution in both coated and uncoated nano-scale $LiFePO_4$ samples upon chemical delithiation has been investigated by this technique. Different kinetic behaviors are observed in the two samples and the technique helps to understand the delithiation mechanism in the nano-scale $LiFePO_4$ and is able to resolve phase evolution in *seconds*' resolution.

1. Introduction

The rate of charging and discharging in battery electrode materials are controlled by interface chemistry and diffusion mechanisms. While the macroscopic polarization behavior of a cell can provide a measure of the macroscopic rates of these processes, few techniques have been developed by which to investigate the mechanisms and kinetics of intercalation phenomena and the effect of these mechanisms on macroscopic rate performance. $LiFePO_4$ is a positive electrode material used in high power rechargeable lithium batteries; its charge (discharge) proceeds with two-phase reaction, leading to the formation of $FePO_4$ ($LiFePO_4$). Conventional $LiFePO_4$ with micron size particles have shown sluggish rate performance due to poor intrinsic electronic conductivity [1–3] and one-dimensional lithium transport path in the bulk [4,5]. Armand and co-workers [6] showed that a carbon coating simultaneously increases the electronic conductivity of this material and prevents particle growth. Meethong et al. [7,8] showed that decreasing the particle size to below 50 nm could significantly extend the solid solutions in the vicinity of $LiFePO_4$ and $FePO_4$, therefore enhancing the lithium mobility. Many studies have been devoted to trying to understand the lithium intercalation/deintercalation mechanism [7–14] and three main proposed mechanisms are summarized in Fig. 1. In an electron microscopy study of $Li_{0.5}FePO_4$ obtained by chemical delithiation, Chen and Richardson [9] showed that in a micro-size platelet-shaped particle, alternating domains of lithium rich and lithium poor phosphate phases with intermediate zones (see Fig. 1a). Mostly recently, Delmas et al. [10] reported a "domino-cascade model" in nano-scale $LiFePO_4$ where the delithiation process is nucleation limited (Fig. 1c), instead of diffusion limited (Fig. 1b). It is believed that the exact mechanism in different samples depends on the size, morphology and surface chemistry of the samples. New coated $LiFePO_4$ particles have been reported with superior rate capability [15], in which a glassy Li-phosphate mixed ion-electron conducting coating is created on the surface of nano-scale particles. In this study we report an investigation of phase evolution in both coated and uncoated nano-scale $LiFePO_4$ upon chemical delithiation by an intermittent X-ray diffraction technique. We demonstrate that this technique is able to resolve phase evolution time differences in the coated and uncoated samples, providing a tool by which structural kinetics can be correlated with the rate performance of various lithium intercalation compounds.

2. Materials and experimental methods

Powders of composition $LiFePO_4$ were provided by Kang and Ceder (Massachusetts Institute of Technology) and the details of the synthesis can be found in another recent publication [15]. One batch of particles was coated with glassy film during synthesis and is designated simply as "coated" within this paper. Particles that were not coated are designated as "uncoated." The particle size of both batches of particles was approximately 50–100 nm.

* Corresponding author. Tel.: +1 3528463320; fax: +1 3528463355.
E-mail address: ysmeng@mse.ufl.edu (Y.S. Meng).

0378-7753/$ – see front matter © 2008 Elsevier B.V. All rights reserved.
doi:10.1016/j.jpowsour.2008.08.055

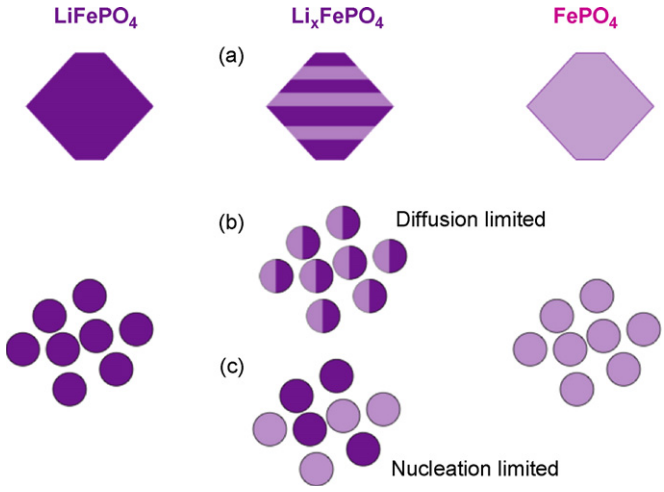

Fig. 1. Schematic illustration of proposed delithiation mechanisms in $LiFePO_4$. Although spherical shape is used to represent the nano-size particles, it should be noted that $LiFePO_4$ with olivine structure has one-dimensional lithium diffusion path.

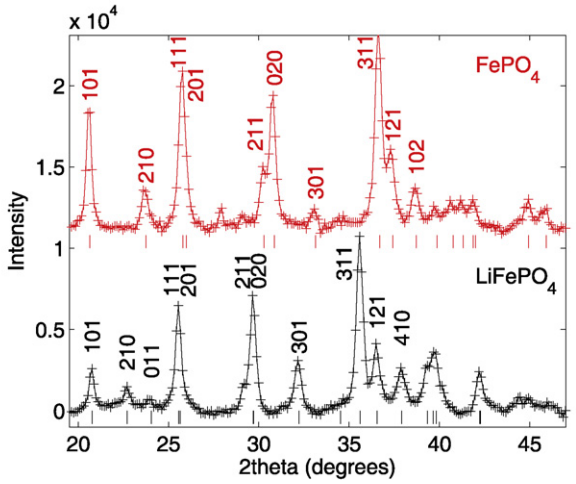

Fig. 2. Typical X-ray diffraction pattern of the coated sample in the lithiated (lower, $LiFePO_4$) and delithiated (upper, $FePO_4$) states. The delithiated state was obtained after a total immersion time of 600 s. Indicated peak positions calculated from orthorhombic Pnmb $LiFePO_4$ and $FePO_4$.

For both types of powders, approximately 0.8 g of powder was uniaxially pressed in a 5 mm diameter pellet die using a force of 3 metric tons. An oxidizing solution was prepared by adding 3 g of NO_2BF_4 to 20 mL of acetonitrile and was manually stirred until the NO_2BF_4 was completely dissolved. Diffraction patterns were collected using an Inel laboratory diffractometer equipped with a 120° curved position sensitive detector (CPS-120). A note should be made regarding the spatial resolution and total number of crystallites sampled in the measurement. The slit size of the diffractometer is approximately 5 mm × 300 μm and this cross-section is incident upon the sample at an angle of 6°. The projected irradiated area on the sample is therefore 5 mm × 2.9 mm, or 14.5 mm^2. Because the crystallite size is on the order of 100 nm, approximately 10^9 crystallites would be sampled at the top surface. Although the sample is highly porous and this reduces the number of crystallites sampled at the top surface, the X-ray penetration depth enables the measurement of a certain thickness of the sample and these two effects are counteracting. It can therefore be stated that approximately 10^9 crystallites are sampled using this technique. An intermittent chemical delithiation experiment was undertaken wherein the powder pellets of $LiFePO_4$ were dipped into the oxidizing solution for a given amount of time (±0.5 s), removed, wiped with a dry cloth, placed into the diffractometer, and a diffraction pattern was collected for 180–300 s. The pellet was then re-immersed in the oxidizing solution and the process was repeated. The $LiFePO_4$ powder reacts with the solution according to the reaction:

$$LiFePO_4 + NO_2BF_4 \rightarrow LiBF_4 + NO_2 + FePO_4. \quad (1)$$

Transmission electron microscope (TEM) images were collected from the pristine powders, suspended on a copper grid with lacey carbon under an accelerating voltage of 200 kV on JEOL 2010F microscope with a field emission source.

3. Results and discussion

An initial diffraction pattern of the $LiFePO_4$ phase prior to sample immersion and the $FePO_4$ phase after a total immersion time of 600 s is shown in Fig. 2. The refined lattice parameters of $LiFePO_4$ are $a = 10.30$ Å, $b = 5.98$ Å and $c = 4.68$ Å and those of $FePO_4$ are $a = 9.87$ Å, $b = 5.83$ Å and $c = 4.82$ Å. XRD patterns are collected over 10–120°, though the most significant differences in the diffraction pattern of the respective phases are apparent in the range $29° < 2\theta < 39°$. For example, the (2 1 1) and (0 2 0) reflections of $LiFePO_4$ are observed at 2θ angles slightly less than 30° and the (2 1 1) and (0 2 0) reflections of $FePO_4$ are observed at 2θ angles slightly greater than 30°. These isolated peaks can be used to discriminate these two phases and/or the fractions of various phases present in a multiphase mixture. Diffraction peaks in the range $35° < 2\theta < 39°$ also show some differences, although some overlap is observed. For example, although the (3 1 1) reflection of the $LiFePO_4$ phase (35.6°) does not overlap with any reflections of the $FePO_4$ phase, the (1 2 1) reflection of the $LiFePO_4$ phase (36.5°) overlaps with the (3 1 1) reflection of the $FePO_4$ phase (36.7°). Thus, with the current resolution, the diffracted intensity at approximately 36.6° cannot be used by itself to discriminate the presence of a particular phase. The peak broadening of the diffraction lines does not change significantly during the chemical delithiation process, consistent with the observation in electrochemical experiment reported by Delmas et al. [10].

Fig. 3 shows a contour plot of partial diffraction patterns ($29° < 2\theta < 39°$) of the uncoated $LiFePO_4$ samples as a function of

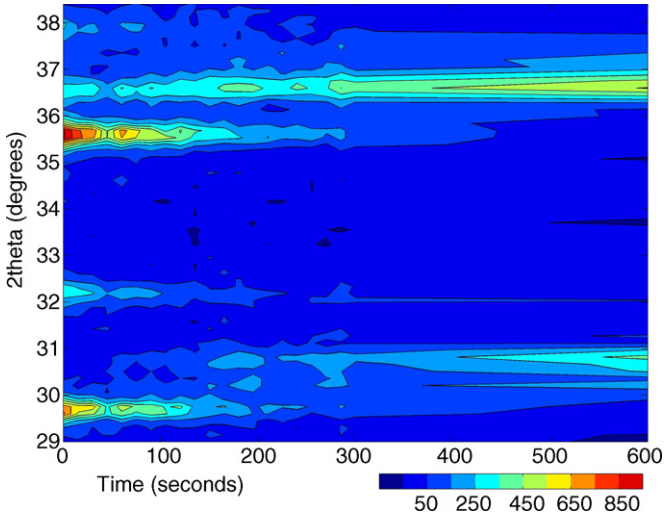

Fig. 3. Contour plot of diffracted intensities in the region $29° < 2\theta < 38.4°$ as a function of immersion time. With increasing immersion time, the diffracted peaks of $LiFePO_4$ (29.7°, 32.2°, 35.6°, 36.5° and 37.9°) decrease in intensity while those of the $FePO_4$ (30.3°, 30.9° and 36.6°) increase intensity.

total immersion time. Between 0 and 300 s, intermittent immersion was conducted for 15 s increments. After a total immersion time of 300 s, the sample was immersed for an additional 300 s and a final diffraction pattern was collected. Fig. 3 demonstrates that a decrease in the intensity of the (0 2 0) reflection of the $LiFePO_4$ phase (29.7°) is apparent with increasing immersion time. This indicates a loss of the $LiFePO_4$ phase with increasing immersion, consistent with the oxidation reaction given by Eq. (1). A similar decrease in intensity is seen in the (3 0 1) reflection of the $LiFePO_4$ phase (32.2°). Correspondingly, there is a consistent increase in the relative intensity of the (2 1 1) (30.3°) and (0 2 0) (30.9°) reflections of the $FePO_4$ phase. In the range $35° < 2\theta < 39°$, similar respective intensity decreases and increases in reflections of the $LiFePO_4$ and $FePO_4$ phases can be seen. As stated previously, the diffracted intensity at 36.6° cannot be attributed to a specific phase using the current resolution. However, the large decrease in intensity of the (3 1 1) reflection at 35.6° can be attributed to the decreasing fraction of the $LiFePO_4$ phase and correlates with the intensity decreases seen in (0 2 0) (29.7°) and (3 0 1) (32.2°) reflections.

To further represent the decreasing intensity of the $LiFePO_4$ phase reflections, the two diffracting peaks of the highest intensity {(0 2 0) at 29.7° and (3 1 1) at 35.6°} were fit to profile shape functions in order to extract the integrated peak intensity. Within the framework of MATLAB (The MathWorks, Inc.), a 6th order polynomial function was first fit to the background and subsequently subtracted from the diffraction patterns. A Gaussian profile shape function was then fit to each of the peaks of interest using a nonlinear least squares method within the *fit* function. The integrated intensities of the (0 2 0) and (3 1 1) reflections of the $LiFePO_4$ phase as a function of total immersion time are shown in Fig. 4. The error bars shown in Fig. 4 are calculated using the 95% confidence intervals extracted from the fitting routine. The outer diagram of Fig. 4, corresponding to the uncoated particles, demonstrates that the diffracted intensity of two reflections of the $LiFePO_4$ phase approaches a minimum value in approximately 200 s of total immersion time.

Equivalent experiments were performed on the coated $LiFePO_4$ particles. During the first diffraction experiment on the coated particles, it was noted that a 15 s immersion time results in a complete disappearance of the $LiFePO_4$ phase reflections. Therefore, immersion increments of 1 s were used for these samples. The changes in integrated intensities for the pellet composed of the coated particles are shown as the inset in Fig. 4. Nearly complete disappearance in the intensity of the $LiFePO_4$ reflections was observed within 3 s of total immersion time. This intermittent immersion and X-ray diffraction experiment demonstrates a clear difference in the phase transformation kinetics of two types of nano-scale $LiFePO_4$ particles.

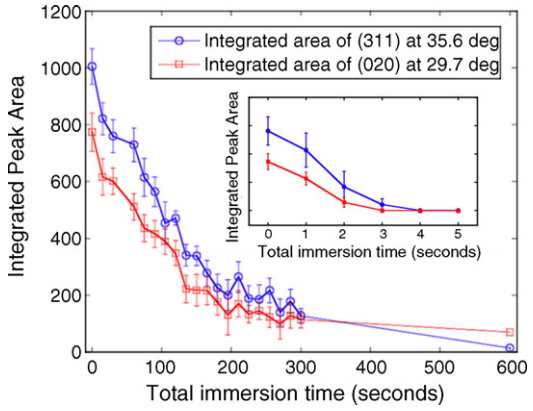

Fig. 4. Change in integrated intensity of the (3 1 1) and (0 2 0) reflections of the $LiFePO_4$ phase as a function of total immersion time. Outer diagram represents the change in intensity of the uncoated powder and the inset represents the change in intensity of the coated power.

The rate of $LiFePO_4 \rightarrow FePO_4$ transformation depends on the rate at which Li^+ ions and electrons can migrate through the solution/powder interface. The difference in the surface characteristics of the two types of powders is revealed in the transmission electron micrographs shown in Fig. 5. Two different surfaces of crystals with different orientations are shown and the distances of lattice planes are measured as 4.7 Å, indicating that these lattice planes are either *ac* plane or *bc* plane. The 3–5 nm surface layer on the coated sample is believed to be a glass mixed ion-electron conducting coating, introduced during the synthesis [14]. The coated sample has shown superior rate performance in a lithium half-cell: 44 C (82 s) discharge with 80% of full capacity; while the uncoated sample cannot deliver little capacity at that rate [15]. The intermittent X-ray diffraction study on the uncoated particle sample demonstrates that $LiFePO_4$ starts disappearing during the first 15 s immersion step and completely disappears after approximately 200 s of total immersion. Inversely, the $FePO_4$ reflections start to appear after about 100 s. In the sample containing coated particles, these events occur in less than 5 s. Consistent with earlier work [11,16–19], it is likely that the surface coating provides a Li^+ ion and electron path to facilitate the oxidation process. Although in principle the chemical reaction and the electrochemical process should lead to the same end phase, some major differences are noticed: in chemical delithiation process, the chemical potential of the oxidant (NO_2^-/NO_2) lies about +2.1 V vs. normal hydrogen electrode (NHE), which means this potential is 5.1 V vs. Li [20]. Therefore, a constant high voltage is set when the powders are immersed in the oxidant. In the electrochemical charge/discharge process, galvanostatic (constant current) mode is applied to access the rate capability of the materials. In addition, in chemical delithiation, the reagents/particle contact can be established easily where electrons and ions are interacting. Thus, while the chemical delithiation time differences observed between the uncoated and coated particles are two orders of magnitude different, these results may not translate directly into the kinetics during electrochemical delithiation. Chemical and electrochemical delithiation are unique processes and may provide unique time-dependent structural results. An *in situ* electrochemical cell is currently being designed to investigate the effects of chemical versus electrochemical delithiation/lithiation processes.

Finally, a few comments are made regarding the intermittent X-ray diffraction approach. The diffractometer used in this experiment hosts a curved position sensitive detector that enables the collection of a 120° range of 2θ simultaneously. Diffraction patterns are therefore collected much faster than in a conventional laboratory diffractometer, i.e. in less than 5 min in this experiment. Thus, many diffraction patterns can be collected during the course of a complete immersion experiment. For example, 21 diffraction patterns were collected on the sample containing the uncoated particles and the resulting large number of data points are reflected in Fig. 4. This large quantity of structural information has been used here to observe differences in transformation time between the coated and uncoated particles of two orders of magnitude. Several potential contributions to the measurable transformation time in an intermittent-type experiment must also be acknowledged. There may exist an initiation time for the chemical delithiation process to initiate which may influence the time-dependence measured through an intermittent approach. To prevent such an effect in the current results, both the coated and uncoated particles were first tested using a 15 s incremental immersion time. Furthermore, the solution temperature, stirring, oxidizer concentration

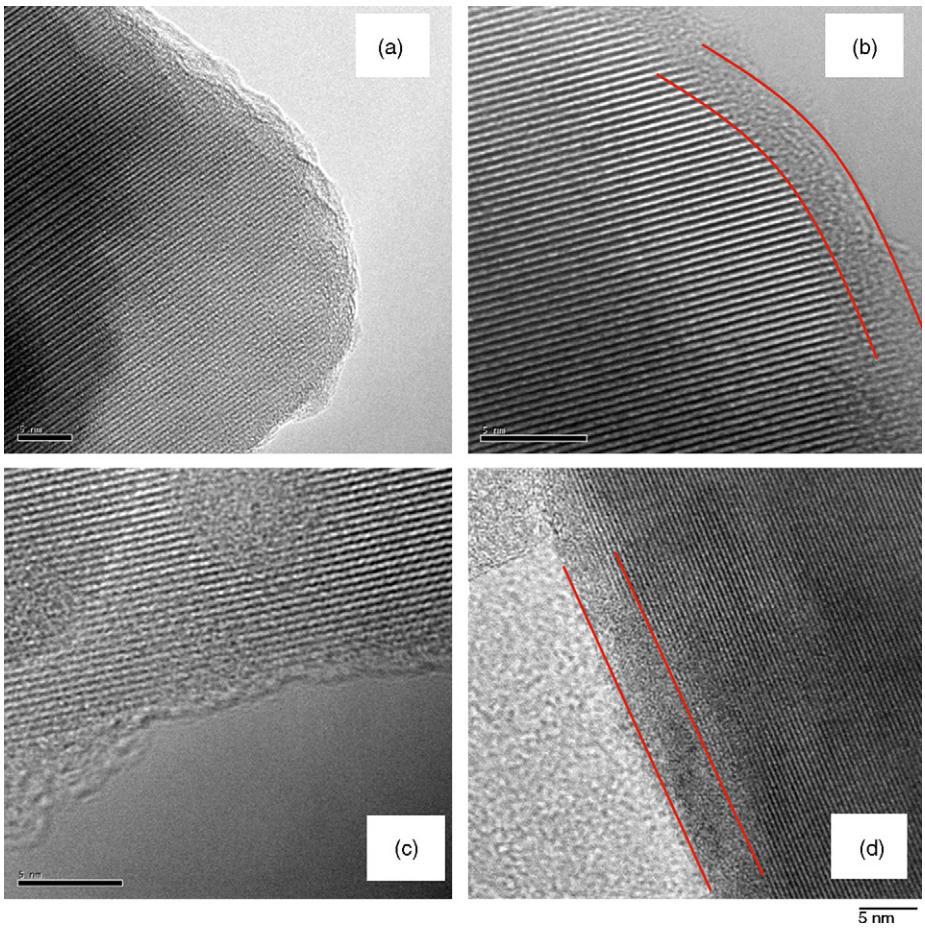

Fig. 5. High-resolution TEM images of (a) and (c) uncoated $LiFePO_4$ and (b) and (d) coated $LiFePO_4$. The coating on the particle is highlighted with solid lines. A thin layer (~3 nm) amorphous-like layer is observed in (b) and (d) (the length bar in each figure represents 5 nm).

and sample compact density may also affect such measurements. However, in this comparison study there was little difference between the oxidizing solution and powder compact preparation of the uncoated and coated specimens, minimizing potential sample and solution effects. [A] new improved technique that collects XRD spectra during a single immersion step is currently underway and a more quantitative analysis will be presented in future publications.

4. Conclusion

Nano-scale $LiFePO_4$ samples with and without coating under chemical delithiation were investigated by a new intermittent X-ray diffraction technique. Different kinetic behaviors are observed in the two samples with delithiation times that are two orders of magnitude different. This in-house, laboratory diffraction technique helps to understand the delithiation mechanism in the nano-scale $LiFePO_4$ and is able to resolve phase evolution in *seconds'* resolution.

Acknowledgments

The authors gratefully acknowledge the technical assistance of Abhijit Pramanick and financial support of the U.S. National Science Foundation through Award DMR-0746902. The authors are also grateful to Mr. B. Kang and Dr. G. Ceder for providing the samples for this work.

References

[1] A.K. Padhi, K.S. Nanjundaswamy, J.B. Goodenough, Journal of the Electrochemical Society 144 (1997) 1188.
[2] C.P. Delacourt, P. Poizot, S. Levasseur, C. Masquelier, Electrochemical and Solid State Letters 9 (2006) A352.
[3] T. Maxisch, F. Zhou, G. Ceder, Physical Review B 73 (2006) 104301.
[4] M.S. Islam, D. Driscoll, C.A.J. Fisher, P.R. Slater, Chemistry of Materials 17 (2005) 5085.
[5] D. Morgan, A. Van der Ven, G. Ceder, Electrochemical and Solid State Letters 7 (2004) A30.
[6] N. Ravet, et al., CA Patent No. EP1049182 (2002).
[7] N. Meethong, H.Y.S. Huang, W.C. Carter, Y.M. Chiang, Electrochemical Solid State Letters 10 (2007) A134.
[8] N. Meethong, H.-Y.S. Huang, S.A. Speakman, W.C. Carter, Y.-M. Chiang, Advanced Functional Materials 17 (2007) 1115.
[9] G. Chen, X. Song, T. Richardson, Electrochemical and Solid State Letters 9 (2006) A295.
[10] C. Delmas, M. Maccario, L. Croguennec, F. Le Cras, F. Weill, Nature Materials 7 (2008) 665.
[11] C. Delacourt, C. Wurm, L. Laffont, J.B. Leriche, C. Masquelier, Solid State Ionics 177 (2006) 333.
[12] A.S. Andersson, B. Kalska, L. Haggstrom, J.O. Thomas, Solid State Ionics 130 (2000) 41.
[13] L. Laffont, et al., Chemistry of Materials 18 (2006) 5520.
[14] V. Srinivasan, J. Newman, Journal of the Electrochemical Society 151 (2004) A1517.
[15] B. Kang, G. Ceder, Battery materials for ultra-fast charging and discharging, submitted for publication.
[16] P.S. Herle, B. Ellis, N. Coombs, L.F. Nazar, Nature Materials 3 (2004) 147.
[17] R. Dominko, et al., Journal of Power Sources 153 (2006) 274.
[18] K.-F. Hsu, S.-Y. Tsay, B.J. Hwang, Journal of Materials Chemistry 14 (2004) 2690.
[19] H. Huang, S.-C. Yin, L.F. Nazar, Electrochemical and Solid-State Letters 4 (2001) A170.
[20] A.R. Wizansky, P.E. Rauch, F.J. Disalvo, Journal of Solid State Chemistry 81 (1989) 203.